第 33 卷第 12 期　　焊　接　学　报　　Vol. 33　No. 12
2012 年 12 月　　TRANSACTIONS OF THE CHINA WELDING INSTITUTION　　December　2012

不锈钢超声 – 脉冲 TIG 焊缝的组织与性能

张勤练，　林三宝，　范成磊，　杨春利
（哈尔滨工业大学 先进焊接与连接国家重点实验室，哈尔滨　150001）

张勤练

摘　要： 超声辅助 TIG 焊是一种新型高效焊接方法. 前期研究中采用的是直流，而实际焊接中多用脉冲. 采用超声辅助脉冲 TIG 焊方法焊接不锈钢 1Cr18Ni9Ti，对焊接接头的组织和性能进行了分析，讨论了焊缝熔深增加、组织细化的机理. 结果表明，施加超声振动后，焊缝熔深增加 1 倍以上，焊缝区组织细化，基值电流期间电弧压缩明显，接头抗拉强度和断后伸长率都有所提高. 分析认为声流力是焊缝熔深增加的主要动力，声空化与声流搅拌的共同作用使焊缝组织细化.

关键词： 不锈钢；超声振动；晶粒细化；力学性能
中图分类号： TG457.11　　**文献标识码：** A　　**文章编号：** 0253 – 360X(2012)12 – 0061 – 04

0　序　　言

为提高 TIG 焊生产效率，近年来出现了许多高效 TIG 焊接方法，如等离子弧焊、活性剂 TIG 焊、双钨极 TIG 焊等. 超声辅助 TIG 焊是近年来由哈尔滨工业大学杨春利教授提出的一种新型焊接方法，该方法能够增加焊缝熔深，细化焊缝组织，提高焊接生产效率[1]. 该方法的关键在于通过焊枪将超声振动施加于电弧空间，与清华大学吴敏生教授[2,3]提出的在焊接回路中耦合高频脉冲信号激励电弧产生超声有着本质的区别.

前期的研究仅停留在直流 TIG 焊上，而实际中不锈钢的焊接多采用脉冲 TIG 焊，因此将超声振动施加到脉冲 TIG 焊中，焊接 1Cr18Ni9Ti 奥氏体不锈钢，研究超声振动对焊接电弧形态及焊接接头组织与性能的影响. 通过与常规脉冲 TIG 焊的对比，分析焊缝组织和力学性能，结合电弧形态讨论超声振动使焊缝熔深增加的原因. 根据超声振动对金属熔体的细化理论分析焊缝组织细化机理.

1　试验方法

试验采用的焊接方法为超声辅助脉冲 TIG 焊，也就是将超声振动施加于常规脉冲 TIG 焊中. 图 1 为超声辅助脉冲 TIG 焊原理示意图. 超声复合焊枪由换能器、超声变幅杆、钨极导电杆、陶瓷喷嘴、气体保护和水冷装置等构成. 超声电源产生高频脉冲信号激励压电陶瓷换能器产生超声振动，超声振动通过变幅杆放大振幅，从变幅杆端部辐射到电弧空间中.

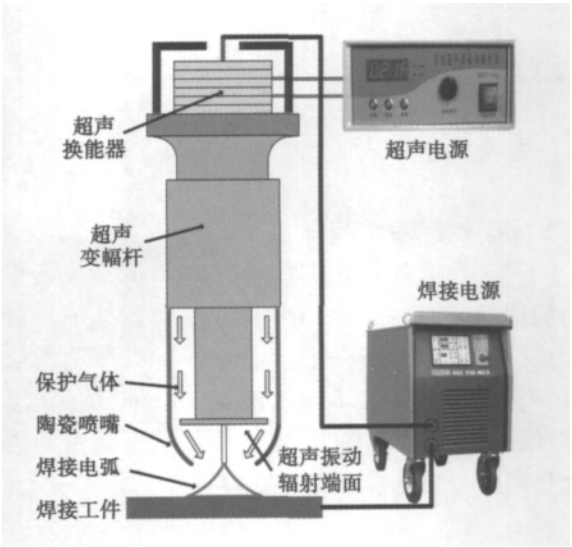

图 1　超声辅助脉冲 TIG 焊原理示意图
Fig. 1　Schematic of ultrasonic-assisted pulse TIG welding

焊接母材为 1Cr18Ni9Ti 奥氏体不锈钢，板厚为 3 mm，图 2 是其微观组织形貌. 从图 2 中看出，焊接母材的组织为等轴奥氏体，在奥氏体基体上存在着细小点状碳化物、氧化物及氮化钛夹杂. 试验中焊接试片尺寸为 100 mm × 60 mm × 3 mm，焊前用砂布轮打磨表面，并用丙酮擦拭，除去表面油污.

收稿日期：2011 – 09 – 28
基金项目：国家自然科学基金资助项目(50975063)

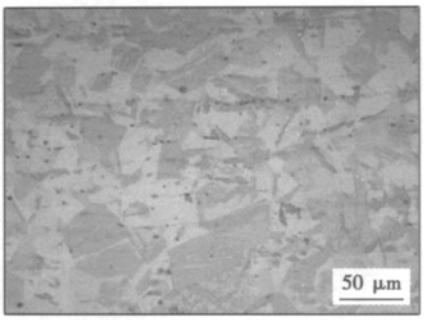

图 2 不锈钢 1Cr18Ni9Ti 母材微观组织

Fig. 2 Micrograph of stainless steel 1Cr18Ni9Ti

在母材上进行重熔试验，观察施加超声前后焊接接头的熔化形式和微观组织形貌；采用填丝对接焊获得接头，对接头进行拉伸性能测试及断口分析；同时采用高速摄像对焊接电弧的形态进行观察.

高速摄像机型号为 CAM-RECORD 5000X2，配有 808 nm 窄带滤光片，拍摄过程中使用频率为 5 000帧/s. 电子万能试验机型号为 INSTRON-5569，拉伸速率为 5 mm/min. 焊接工艺参数如表 1 所示.

表 1 焊接工艺参数

Table 1 Parameters of welding test

试验	峰值电流 I_p/A	基值电流 I_b/A	脉冲频率 f/Hz	脉冲时间 T_p/ms	焊接速度 v/(mm·min^{-1})
堆焊	200	40	6	92	60
对接	190/210	40	6	92	60

2 试验结果与分析

2.1 焊接接头的熔化形式

图 3 为超声振动施加前后脉冲 TIG 焊平板重熔后的截面形貌. 从图 3 中可见，超声振动加入后使焊道熔宽由 9.4 mm 变化为 10.4 mm，熔宽增加约 11%；焊道熔深由 1.5 mm 增加至 3 mm，熔深增加 1 倍. 熔深增加程度较大，焊道的熔化形式由周边熔化型向中心熔化型转变.

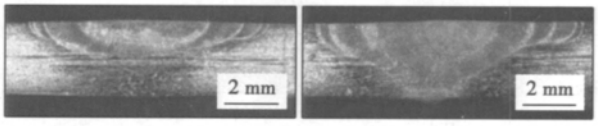

(a) 不施加超声振动 (b) 施加超声振动

图 3 平板重熔截面形貌

Fig. 3 Cross sectional macrographs of remelting plates

2.2 焊接接头的微观组织

图 4 为施加超声振动前后脉冲 TIG 焊缝底部的微观组织. 从图 4a 可见，焊缝底部的组织为胞状树枝晶，胞状树枝晶的生长方向指向焊缝中心，与散热方向相反，δ-铁素体呈骨架状；从图 4b 可见，施加超声振动后，焊缝底部的组织也为胞状树枝晶，胞状树枝晶的生长没有固定方向，δ-铁素体呈蠕虫状与骨架状混合形态，树枝晶尺寸较小. 可见超声振动对焊缝底部的搅拌作用较强，使焊缝底部组织细化，并且使枝晶生长方向改变.

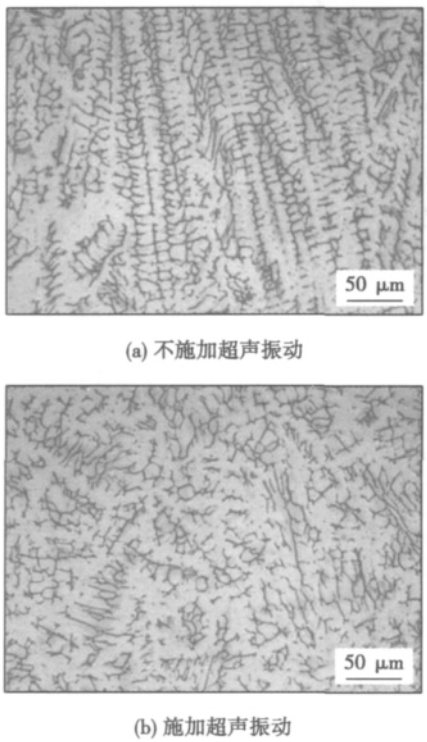

(a) 不施加超声振动

(b) 施加超声振动

图 4 脉冲 TIG 焊缝底部微观组织

Fig. 4 Micrographs of weld bottom by pulse TIG welding

为更加准确地反映超声振动作用下焊缝的组织特点，沿焊接方向将焊缝切开，观察焊缝纵向截面的微观组织形貌. 图 5 为施加超声振动前后脉冲 TIG 焊缝纵向截面的微观组织形貌.

从图 5a 可见，未施加超声振动时，两个凝固熔池之间的组织为胞状树枝晶，生长方向基本垂直于两个点状熔池的交界线，树枝晶较发达，δ-铁素体呈骨架状；从图 5b 可见，施加超声振动后，胞状树枝晶变得细小，δ-铁素体呈骨架状与蠕虫状混合形态，并且在胞状树枝晶的前沿出现了等轴晶. 可见超声振动的加入改变了焊缝微观组织形态.

2.3 力学性能与断口分析

对焊接好的试片取样进行拉伸性能测试，每个焊接参数取三个拉伸试样，取其均值作为最后的抗拉强度与断后伸长率. 拉伸断口均为典型的杯椎状断口，属塑性断裂，拉伸试样的断裂位置均位于焊缝

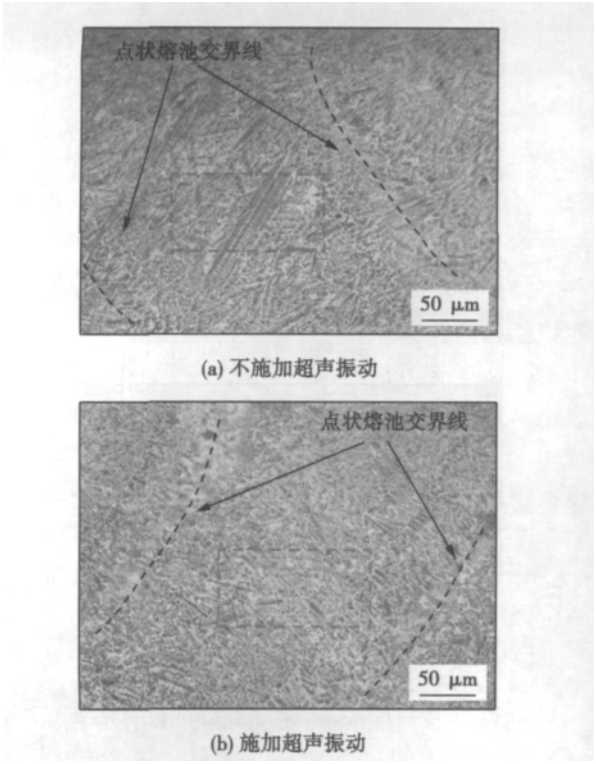

图 5　焊缝纵向截面显微组织形貌

Fig. 5　Micrographs of longitudinal section of weld

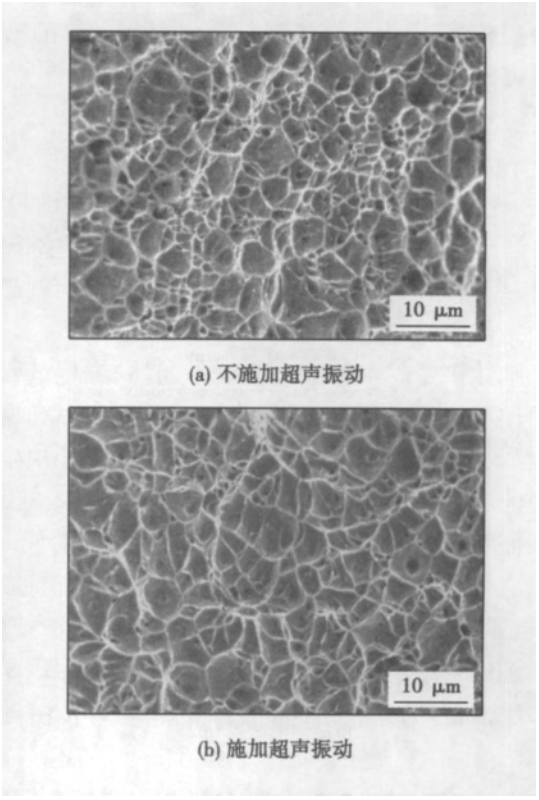

图 6　拉伸试样扫描断口微观形貌

Fig. 6　SEM fractographs of tensile samples

上. 表 2 是拉伸性能的测试结果. 从测试结果看，超声振动的加入提高了焊接接头的抗拉强度和断后伸长率.

表 2　拉伸测试结果

Table 2　Tensile test results

拉伸试件	抗拉强度 R_m/MPa	断后伸长率 A(%)
母材	572.5	53.75
不施加超声振动	539.3	40
施加超声振动	562.3	43.3

图 6 为超声振动施加前后接头拉伸试样扫描断口微观形貌. 对比图 6a，b 可见，拉伸试样断口形貌均为韧窝，断裂方式为塑性断裂；不加超声振动时，断口形貌为较大的等轴韧窝上分布着一些较小的韧窝；施加超声振动后，断口形貌均是较大的等轴韧窝，小韧窝较少，韧窝普遍较深，可见第二相质点.

2.4　电弧形态观察

对超声辅助直流 TIG 焊的研究[4] 表明，当超声振动作用于焊接电弧时，电弧压缩，同时熔池的熔化形式由周边熔化型转变为中心熔化型，认为电弧压缩是熔深增加的驱动力.

在脉冲 TIG 焊中，电弧形态按着脉冲频率周期性地变化，电弧上方的超声振动是否依然能够对电弧产生作用是值得考虑的问题. 利用高速摄像拍摄了平板重熔试验中脉冲 TIG 焊电弧的形态. 图 7 为施加超声振动前后脉冲 TIG 焊电弧的典型形态.

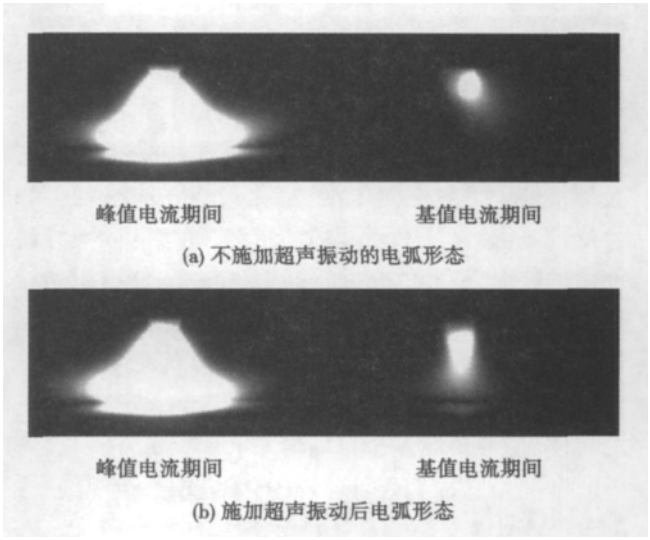

图 7　施加超声振动前后脉冲 TIG 焊电弧形态

Fig. 7　Arc shape of pulse TIG welding with and without ultrasonic vibration

对比图 7a，b 可见，在峰值电流期间，施加超声振动前后电弧形态基本不变；在基值电流期间，施加超声振动后电弧挺度明显提高，消除了电弧偏吹，电弧形态呈锥形，弧柱区面积增加，能量更加集中. 从电弧形态变化看，超声振动在脉冲电流基值期间作

用效果较强，对电弧压缩明显，这与在直流 TIG 焊中的电弧形态不同.

3 讨 论

超声振动施加到脉冲 TIG 焊中，使焊缝熔深增加、组织细化，提高了焊缝的力学性能. 下面就超声振动的作用机理进行讨论.

脉冲 TIG 焊中基值电流较小，起到维持电弧燃烧的作用，当基值电流到来时，电弧空间温度急剧下降，点状熔池迅速凝固，因此峰值电流的大小决定了焊缝的熔深和熔宽，所以焊缝熔深的增加应该发生在峰值电流期间或者峰值电流刚刚结束的瞬间. 从前面电弧形态观察结果看，在脉冲峰值电流持续期间，电弧压缩不明显，因此电弧形态的改变对焊缝熔深增加的贡献不大. 认为焊缝熔深增加的原因是超声振动通过电弧等离子体传播进入到焊接熔池的缘故.

由于奥氏体不锈钢液体粘度较大，超声波在焊接熔池中会产生衰减，形成声压梯度[5]. 声压梯度的形成使得熔池内所受到的压力不同，熔池表面压力较大，熔池内部压力较小，因此形成了声流力，声流力指向熔池的底部. 声流力的存在改变了原有熔池的流动形式，使熔池向下挖掘，因而能增加焊缝熔深.

关于超声振动使组织细化的机制目前主要有三种解释[6-8]，分别是超声空化破碎作用、过冷生核理论、声流搅拌作用. 超声空化破碎作用是指超声在金属液体中产生空化气泡，空化气泡在崩溃时会产生局部高温、高压和强烈的冲击波，能熔断固液界面前沿的枝晶，破碎的枝晶提高了生核率，使组织晶粒细化. 过冷生核理论认为，空化气泡长大时，产生局部过冷，使临界形核半径减小，增加了形核几率. 声流搅拌作用能使熔体的温度场均匀化，能加速对流与传质，使形核质点分布均匀.

在超声脉冲 TIG 复合焊中，焊缝中心组织细小，δ-铁素体呈蠕虫状，认为空化作用的贡献较大. 因为焊缝中心温度梯度较小，凝固缓慢，熔池持续时间较长，为过冷形核提供了足够的时间和空间.

焊缝底部组织为细小的胞状树枝晶，认为超声声流作用的贡献较大. 焊缝底部温度梯度较大，凝固较快，固液界面区域很快进入到半凝固状态，空化作用变得微弱，而超声波在固液界面因衰减而产生的声流力会冲刷刚刚生长的枝晶，使焊缝底部的胞状枝晶变得细小，同时声流的搅拌作用使温度分布均匀化，导致胞状树枝晶的前沿出现部分等轴晶.

4 结 论

(1) 脉冲 TIG 焊中超声振动的施加能增加焊缝熔深，细化焊缝组织，在基值电流期间使电弧明显压缩.

(2) 超声振动的施加提高了焊接接头的抗拉强度和断后伸长率.

(3) 声流力是熔深增加的主要原因，焊缝组织细化是超声空化与声流搅拌共同作用的结果.

参考文献：

[1] 范阳阳，孙清洁，杨春利，等. 基于超声振动的 304 不锈钢 TIG 焊接[J]. 焊接学报，2009，30(2)：91－94.
Fan Yangyang，Sun Qingjie，Yang Chunli，*et al*. TIG welding of the stainless steel 304 based on the ultrasonic vibration [J]. Transactions of the China Welding Institution，2009，30(2)：91－94.

[2] 吴敏生，段向阳，李路明，等. 电弧超声的激发及其特性研究[J]. 清华大学学报(自然科学版)，1999，39(6)：110－112.
Wu Minsheng，Duan Xiangyang，Li Luming，*et al*. Study of arc-ultrasonic excitation and its characteristics [J]. Journal of Tsinghua University (Science and Technology)，1999，39(6)：110－112.

[3] 胡 星，郝红伟，文雄伟，等. 影响电弧超声激发强度的参数[J]. 焊接学报，2007，28(4)：73－76.
Hu Xing，Hao Hongwei，Wen Xiongwei，*et al*. Factors influenced arc-excited ultrasonic intensity [J]. Transactions of the China Welding Institution，2007，28(4)：73－76.

[4] Sun Qingjie，Lin Sanbao，Yang Chunli，*et al*. The arc characteristic of ultrasonic assisted TIG welding [J]. China Welding，2008，17(4)：52－57.

[5] Zhang Songli，Zhao Yutao，Cheng Xiaonong，*et al*. High-energy ultrasonic field effects on the microstructure and mechanical behaviors of A356 alloy [J]. Journal of Alloys and Compounds，2009(470)：168－172.

[6] Jian X，Xu H，Meek T T，*et al*. Effect of power ultrasound on solidification of aluminum A356 alloy [J]. Materials Letters，2005(59)：190－193.

[7] 郭 峰，罗沛兰，毕 秋，等. 金属熔体超声细化处理技术的研究进展[J]. 金属材料与冶金工程，2008，36(1)：59－63.
Guo Feng，Luo Peilan，Bi Qiu，*et al*. Review on metal melt treatment technology using with ultrasonic field [J]. Metal Materials and Metallurgy Engineering，2008，36(1)：59－63.

[8] Cui Y，Xu C L，Han Q. Effect of ultrasonic vibration on unmixed zone formation [J]. Scripta Materialia，2006(55)：975－978.

作者简介： 张勤练，男，1986 年出生，博士研究生. 主要研究方向为高效化焊接方法与质量控制. 发表论文 1 篇. Email：zhangqinlian052@126.com

通讯作者： 林三宝，男，副教授，博士研究生导师. Email：sblin@hit.edu.cn

Mechanical Engineering, Zhengzhou 450001, China; 2. School of Material Science and Engineering, Zhengzhou University, Zhengzhou 450001, China). pp 57 - 60

Abstract: The purity of the brazing alloys is necessary to be improved with the increasing cleanness of steel. This paper aims at investigating the influence of trace calcium that is contained in filler metal during production process. The melting property, microstructure and spreading performance of BAg45Cu30Zn alloy with various calcium additions have been studied, by employing simultaneous thermal analyzer and scanning electron microscope. The results show that the solidus temperature increases, the liquidus temperature decreases and the melting range narrows, with the calcium content increasing in alloy. The element calcium in the form of CaO exists as the crystal nucleus to refine alloy microstructure. The spreading performance of alloy on 316LN stainless steel has been weakened, resulting from the existence of calcium element.

Key words: trace calcium; AgCuZn brazing alloy; melting property; microstructure; spreading performance

Microstructure and mechanical behaviors of stainless steel weld metal by ultrasonic assisted pulse TIG welding technology ZHANG Qinlian, LIN Sanbao, FAN Chenglei, YANG Chunli (State Key Laboratory of Advanced Welding and Joining, Harbin Institute of Technology, Harbin 150001, China). pp 61 - 64

Abstract: Ultrasonic assisted TIG welding is a new technology with high efficiency. In previous study, direct current was used. However, pulse current was expected in actual welding production. In this study, ultrasonic assisted pulse TIG welding technology was applied to weld 1Cr18Ni9Ti austenitic stainless steel. Microstructure and mechanical properties of the joints were analyzed. The reasons for weld penetration increasing and microstructure refinement were discussed. Experimental results indicated that the welding penetration with ultrasonic vibration was double of that without it. The microstructure of the weld zone was refined and the arc shape was compressed in base current period. The ultimate tensile strength and elongation were higher than that without ultrasonic vibration. Weld penetration increasing is perhaps attributed to acoustic streaming as the main driving force. The refinement of microstructure may be caused by the corporate effects of acoustic cavitation and acoustic streaming.

Key words: stainless steel; ultrasonic vibration; grain refinement; mechanical property

Study on life-prediction of solder joint under combined loading WANG Huan, YANG Ping, XIE Fangwei, XI Tao (School of Mechanical Engineering, Jiangsu University, Zhenjiang 212013, China). pp 65 - 68

Abstract: A life-prediction approach of solder joints under combined thermal and vibration loading is provided in this paper. The deformations of solder joints are calculated respectively under vibration and thermal cycling loading based on finite element method. The calculated results are defined as boundary conditions of the multiaxial loading to investigate the strain/stress of the solder joints. Then the life of solder joints is calculated. The result reveals that the life of solder joints can be divided into three regions according to the vibration amplitude at the same temperature: the life of solder joints in region Ⅰ is affected by thermal loading; that in region Ⅱ is greatly affected by the combined loading; that in region Ⅲ is affected by the vibration amplitude. The trend of the simulation results basically agrees with that of the test results.

Key words: solder joints; combined loading; life-prediction

Analysis for microstructure and mechanical property of Sn-3Ag-0.5Cu solder joints in high density LED packages WANG Xinxin[1], LIU Jianping[1], GUO Fu[1], LIU Li[2], LEI Yuanhong[2] (1. College of Materials Science and Engineering, Beijing University of Technology, Beijing 100124, China; 2. R&D Center, Beijing Leyard Electronic Science Technology Co., Ltd, Beijing 100091, China). pp 69 - 72

Abstract: The microstructure of Sn37Pb and Sn3Ag0.5Cu solder joints under as-reflowed and isothermal aged conditions were observed respectively. The shear strength of samples were also measured. The results suggested that despite the IMC layer of the Sn37Pb solder joints was thicker than the Sn3Ag0.5Cu solder joints, both of them were within the acceptable range. The Sn3Ag0.5Cu solder joints shows a bigger shear strength due to its special structure of β-Sn primary crystal coated by reticular eutectic. Besides, the shear strength of the two solder joints decreased after aging. Although lead-free solder is the inevitable trend to the development of electronic packaging industry instead of Sn37Pb solder, precision reflowing process still plays an important role to improve the quality of the solder joints.

Key words: LED package; eutectic solder alloys; microstructure; shear strength

Spectrum analysis of A-TIG welding for aluminum alloy YAN Keng[1], YANG Gang[1], ZHAO Yong[1], GAO Lihua[1], LU Jiansheng[2] (1. Provincial Key Lab of Advanced Welding Technology, Jiangsu University of Science Technology, Zhenjiang 212003, China; 2. Shanghai Waigaoqiao Shipbuilding Co., Ltd, Shanghai 200137, China). pp 73 - 76, 105

Abstract: A-TIG welding experiments were conducted by using five species of single-component activating fluxes, including SiO_2, TiO_2, CaF_2, Cr_2O_3, $BaCl_2$ and complex formulation YG304. The spectrum in A-TIG welding process is tested by spectrometer. The distribution law of flux element in arc space is analyzed. The experimental results indicate that the above activating fluxes have different effects on weld penetration. The most remarkable increasing is obtained when the flux is YG304. The spectral lines of argon atom and aluminum atom are the main spectral lines of the A-TIG welding arc. Different cross-spectrum distribution of arc is presented with different fluxes. The increasing of penetration may be attributed to the recombination of positive ions such as Si^{4+}, Ti^{4+}, Cr^{3+} and electron that generates from Ar arc, thus raise the arc temperature and arc force, and ultimately the weld penetration increases. The effect of increased penetration is due to various physical properties of positive ion.

Key words: aluminum alloy; A-TIG; cross-spectrum; weld penetration